

AD-A091 295 DREXEL UNIV PHILADELPHIA PA DEPT OF CHEMISTRY
INFRARED EMISSION BY AN AEROSOL CLOUD. (U)

F/G 7/4

OCT 80 R A MACKAY

DAAG29-79-C-0068

UNCLASSIFIED

NL

ARO-16065.1-C

END
DATE
FILED
12 80
DTIC

UNCLASSIFIED
SECURITY CLASSIFICATION OF THIS PAGE (When Data Entered)

18

(19)
ARO/16065.1-C

REPORT DOCUMENTATION PAGE

READ INSTRUCTIONS
BEFORE COMPLETING FORM

1. REPORT NUMBER

2. GOVT ACCESSION NO.

3. RECIPIENT'S CATALOG NUMBER

AD-A091295 9

4. TITLE (and Subtitle)

6 Infrared Emission By An Aerosol Cloud

5. TYPE OF REPORT & PERIOD COVERED
Final Report
1 Jul 78 - 30 June 80

7. AUTHOR(s)

10 Raymond A. Mackay

8. CONTRACT OR GRANT NUMBER(S)

DAAG29-78-G-0117
DAAG29-79-C-0068

9. PERFORMING ORGANIZATION NAME AND ADDRESS
Department of Chemistry
Drexel University
Philadelphia, PA 19104

10. PROGRAM-ELEMENT, PROJECT, TASK AREA & WORK UNIT NUMBERS
DAAG29-78-G-0117

11. CONTROLLING OFFICE NAME AND ADDRESS

U. S. Army Research Office
Post Office Box 12211
Research Triangle Park, NC 27709

12. REPORT DATE

11 17 Oct 80

13. NUMBER OF PAGES

14. MONITORING AGENCY NAME & ADDRESS (If different from Controlling Office)

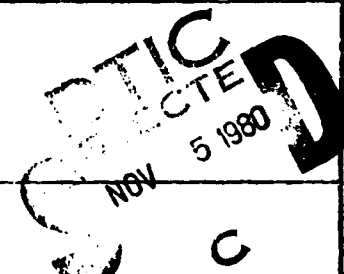
12/24 LEVEL

15. SECURITY CLASS. (of this report)

Unclassified
15a. DECLASSIFICATION/DOWNGRADING SCHEDULE

16. DISTRIBUTION STATEMENT (of this Report)

Approved for public release; distribution unlimited.



17. DISTRIBUTION STATEMENT (of the abstract entered in Block 20, if different from Report)

NA

18. SUPPLEMENTARY NOTES

The view, opinions, and/or findings contained in this report are those of the author(s) and should not be construed as an official Department of the Army position, policy, or decision, unless so designated by other documentation.

19. KEY WORDS (Continue on reverse side if necessary and identify by block number)

Aerosols, Gas-Aerosol Reaction, Infrared Emission

20. ABSTRACT (Continue on reverse side if necessary and identify by block number)

The present study was designed to produce infrared emission by means of exothermic reaction between a gas and a liquid aerosol. We have examined a number of gas-aerosol systems employing acid-base reactions, and have observed significant levels of radiation from the reaction of chlorosulfonic acid aerosol with gaseous ammonia and water. Other systems, including sulfuric acid-ammonia, octanoic acid-ammonia and octylamine-hydrogen chloride, have produced detectable levels of radiation. Some methods for the investigation of emission from gas-aerosol reactions have been explored, and the results of these studies utilizing a chloro-

DD FORM 1 JAN 73 1473 EDITION OF 1 NOV 65 IS OBSOLETE sulfonic aerosol system are presented.

UNCLASSIFIED

409282

8CII 03 063

**INFRARED EMISSION BY AN
AEROSOL CLOUD**

**Final Report
by
Raymond A. Mackay**

10 October 1980

U. S. Army Research Office

**DAAG29-78-G-0117
DAAG29-79-C-0068**

**Department of Chemistry
Drexel University
Philadelphia, PA. 19104**

**Approved For Public Release:
Distribution Unlimited**

TABLE OF CONTENTS

| | <u>Page</u> |
|--|-------------|
| LIST OF FIGURES | (ii) |
| LIST OF TABLES | (ii) |
| INTRODUCTION | 1 |
| RESULTS AND DISCUSSION | 2 |
| General Considerations | 2 |
| Aerosol Generation and Detection | 3 |
| Screening Studies | 7 |
| Reactor System | 9 |
| Gas-Aerosol Reactions | 13 |
| Infrared Spectral Studies | 17 |
| SUMMARY | 20 |

Accession For
NTIS GRA&I
DTIC TAB
Unannounced
Justification

Review
Distribution/
Availability Codes
Area Under
Distr Special

A

LIST OF FIGURES

| | <u>Page</u> |
|--|-------------|
| Figure 1. Dependence of cloud temperature change on time | 4 |
| Figure 2. Aerosol flow system | 5 |
| Figure 3. Concentration of H_2SO_4 <u>vs.</u> pH | 6 |
| Figure 4. Reaction vessels | 8 |
| Figure 5. Reaction of ClSO_3H with $\text{NH}_3/\text{H}_2\text{O}$ and H_2O in vessel A | 10 |
| Figure 6. Gas-aerosol reaction tubes | 11 |
| Figure 7. Schematic diagram of reaction system | 12 |
| Figure 8. Radiometer reading (R) <u>vs.</u> probe temperature (T) for closed and open tubes | 14 |
| Figure 9. Radiometer response <u>vs.</u> time for $\text{NH}_3/\text{H}_2\text{O} - \text{ClSO}_3\text{H}$ gas-aerosol reaction..... | 15 |
| Figure 10. (a). Cell for obtaining infrared spectra of an aerosol stream | 18 |
| (b). Infrared spectrum of DBP neat liquid and aerosol..... | 18 |

LIST OF TABLES

| | |
|---|-------|
| Table I. Reactions and Conditions | 12-13 |
| Table II. Gas-Aerosol Reaction Systems | 14 |

INTRODUCTION

Infrared radiation in the atmosphere above normal background levels can be produced in a variety of ways. For example, combustion gases can produce significant amounts of radiation in the infrared region (2-20 μm). However, the total mass of material, and thus the radiant emittance, is small. In addition, the gas cloud rapidly cools and disperses. In order to significantly increase the amount of airborne material, an aerosol must be employed.

The objective of this work is to investigate the feasibility of producing an aerosol which will emit infrared radiation above normal background levels. Specifically, we are investigating the use of gas-aerosol reactions for this purpose. The first year of this study is described in the proceedings of the first CSL Scientific Conference on Obscuration and Aerosol Research (September 1979). In this stage, infrared emission was observed to result from the reaction of a chlorosulfonic acid aerosol with ammonia and/or water vapor. In the second year these initial feasibility studies were continued and experimental methods which can be applied to this type of investigation were explored. These results are reported in the proceedings of the second CSL Conference (July 1980). This report is a composite covering the period July 1, 1978 - June 30, 1980. The work was supported during this period by the U. S. Army Research Office under grant DAAG29-78-G-0117 and contract DAAG29-79-C-0068.

RESULTS AND DISCUSSION

General Considerations: The rate of the gas-aerosol reaction will be liquid phase controlled; i.e., controlled either by the rate of diffusion in the liquid drop or by the bulk reaction rate. Typically, this will involve reaction rates V_s of $3 \times 10^{-7} - 3 \times 10^{-8}$ moles $\text{cm}^{-2} \text{s}^{-1}$ for 1μ drops, although faster rates are possible. The aerosol will cool rapidly by conduction to the surrounding air such that a steady-state between the rate of heat generation by reaction (q_s) and heat loss by conduction (q_c) should be rapidly ($\sim 30\mu\text{s}$) achieved. Thus, the temperature of the aerosol drops (T_d) and surrounding air in the aerosol cloud (T_c) should be given by eqn (i),

$$T_d = T_c + r V_s \Delta H_s / \kappa_g \quad (i)$$

where r , ΔH_s and κ_g are the drop radius, heat of reaction, and thermal conductivity of the air, respectively. For the above conditions and a ΔH_s of 100 kcal mole $^{-1}$, $\Delta T = T_d - T_c$ should only be a few hundredths of a degree. Further, if we take an idealized model of the aerosol cloud as a sphere of radius R (e.g., 10 m), then the cloud as a whole should lose heat principally by radiation (neglecting convection and treating the cloud as a blackbody). Under these conditions, the rate at which the cloud heats up is given by the rate of heat generation by the drops less the radiation loss (Q_r), as given by equation (ii)

$$N V_c \dot{q}_s = M_c C_c \frac{dT_c}{dt} + \dot{Q}_r \quad (ii)$$

Here, N , V_c , M_c , C_c and t are the aerosol number density, cloud volume, cloud air mass, air heat capacity, and time, respectively. For a blackbody, $\dot{Q}_r = 16 \pi R^2 \sigma T_o^3 (T_c - T_o)$, where σ and T_o are Stefan's constant and the ambient air temperature, respectively. For a constant reaction rate, $\dot{q}_s = 4 \pi r^2 V_s \Delta H_s$.

$$T_c = T_o + \frac{N V_c r^2 V_s \Delta H_s}{4 \sigma R^2 T_o^3} [1 - \exp \left(\frac{-16 \pi R^2 \sigma T_o^3 t}{M_c C_c} \right)] \quad (iii)$$

Equation (iii) is valid for $0 \leq t \leq t_r$, where t_r is the amount of time required for complete reaction of the aerosol. For an aerosol of number density 10^6 cm^{-3} and bulk liquid control, $t_r \sim 10 \text{ sec}$. The entire mass of aerosol can be consumed if the reactive gase constitutes $\lesssim 0.3\%$ by weight of the entire air mass of the cloud. The maximum temperature rise is about 12°C , which is equal to that calculated by assuming that all of the heat of the reaction is deposited in the cloud with no loss. This is so because the radiative loss by the cloud has a lifetime τ of about 10 minutes and is thus small compared with t_r . A sketch of this expected (idealized) behavior is shown in figure 1.

Aerosol generation and detection. A number of candidate gas-aerosol reaction systems were examined for possible use as radiation models. A schematic of the flow system is given in figure 2. The gas and aerosol are combined in a reaction vessel, the temperature measured with a thermistor and the emitted radiation with a radiometer. The radiometer is a Molelectron pyroelectric radiometer model PR200 with a response time of 3 sec for $20 \mu\text{W cm}^{-2}$ full scale, a 0.1 Sr field of view, and a detector area of 0.2 cm^2 . The closed tube (vide infra) and the radiometer are fitted with a KRS-5 window which has a cutoff at about 50μ . Thus, essentially all of the emitted radiation is collected. The thermistor probes (YSI series 400) have a time response of 4-5 sec and a tolerance for exchange of probes of 0.1°C . The meter currently used gives readings to within $\pm 0.3^\circ\text{C}$.

We have been able to generate aerosols of all of the liquids employed to date using a condensation-type generator. However, a compressed air nebulizer (DeVilbis) was used for most of the screening. This generator produces a polydisperse aerosol, but is more convenient to use.

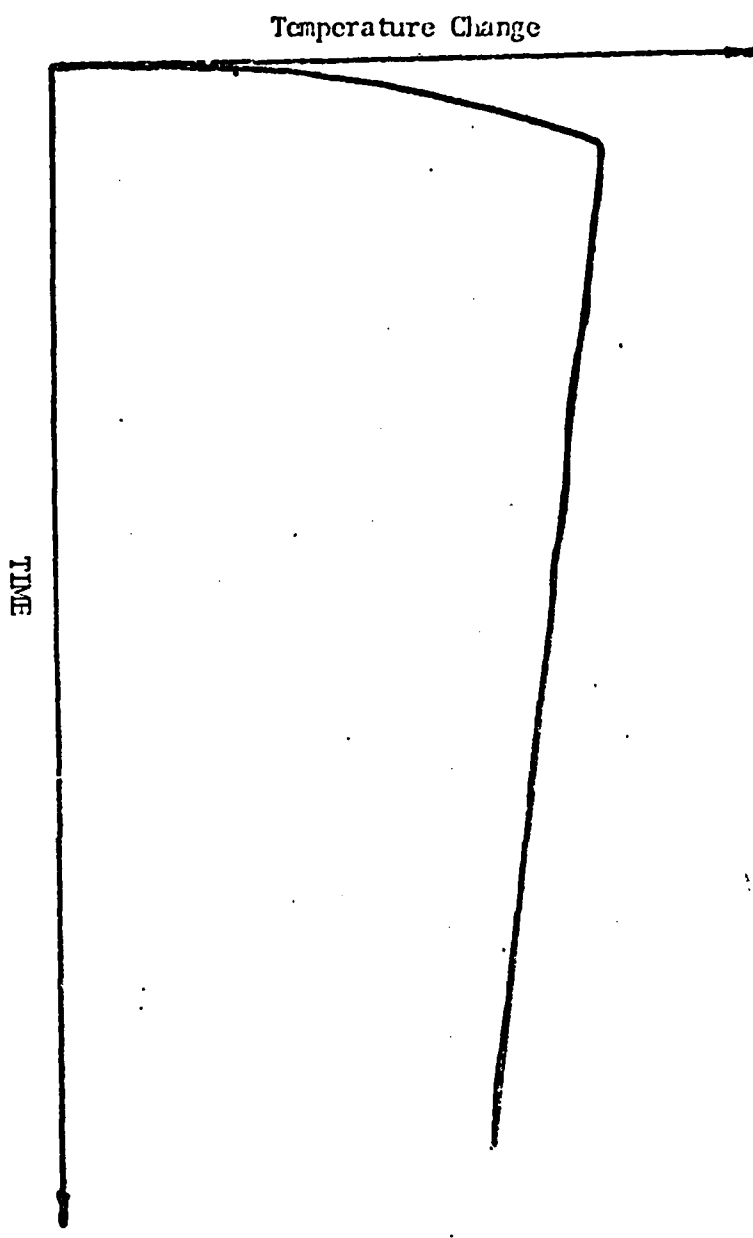
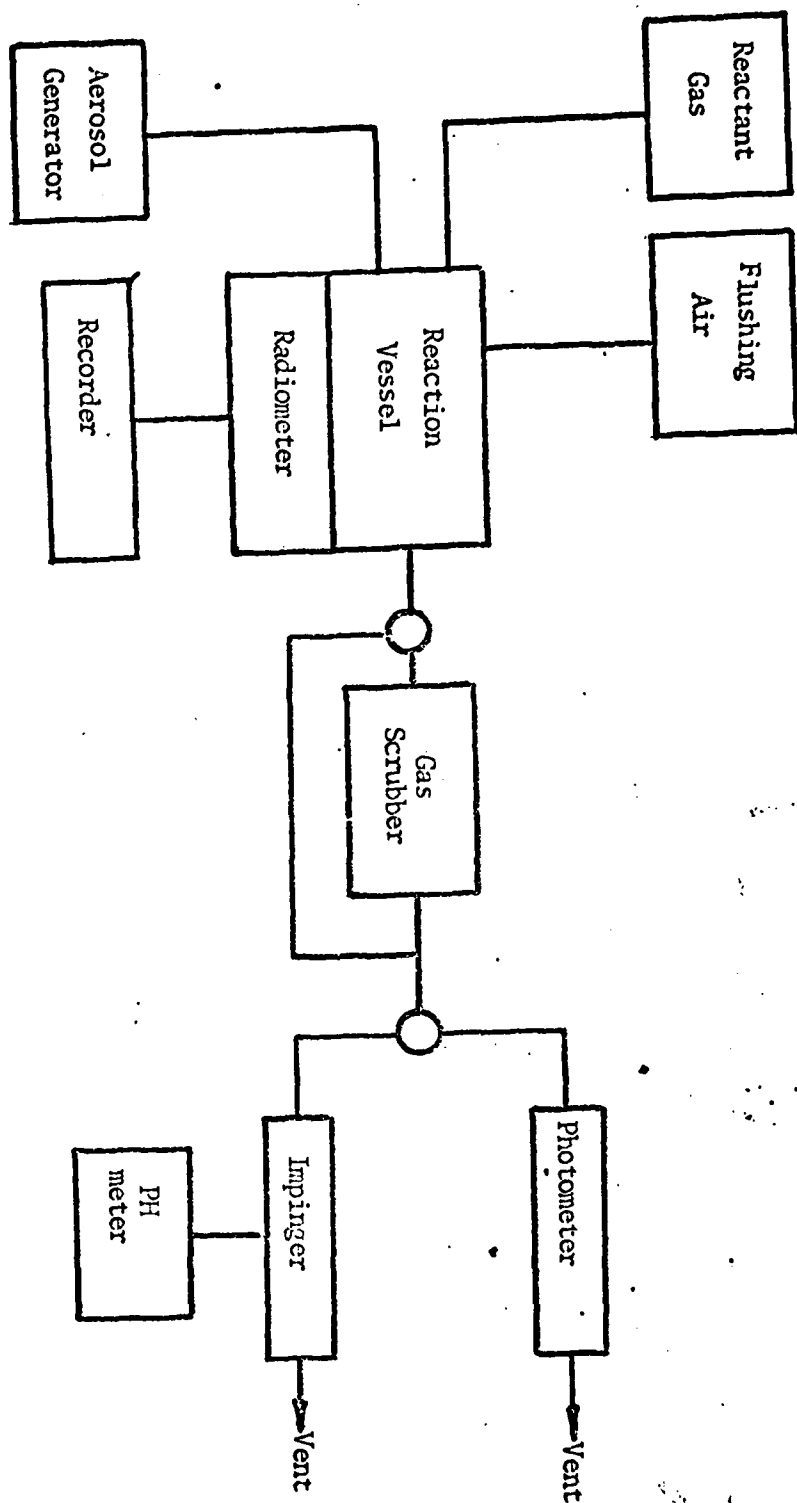


Figure 1. Dependence of cloud temperature change on time according to equation (iii).



(5)

Figure 2. Aerosol flow system. Approximate flow rates are; gas ($0.5 - 1 \text{ l min}^{-1}$), aerosol ($2-3 \text{ l min}^{-1}$) and flushing air (1 l min^{-1}).

The output of the generator is determined by collection for a period of time, normally 1 min, followed by analysis. Nonreactive test aerosol (e.g. - dibutylphthalate) is collected on a millipore filter ($\sim 1 \mu$) and weighed. The acid aerosols are collected in an impinger containing about 100 ml of water and then titrated either coulometrically or with NaOH to a phenolphthalein endpoint. It is also possible, for continuous monitoring, to use a glass pH electrode. A calibration curve for H_2SO_4 is shown in Figure 3. Molecular sieve is employed when necessary to remove the reactant gas from the aerosol stream prior to analysis. The aerosol may be monitored continuously using a Sinclair-Phoenix light scattering photometer.

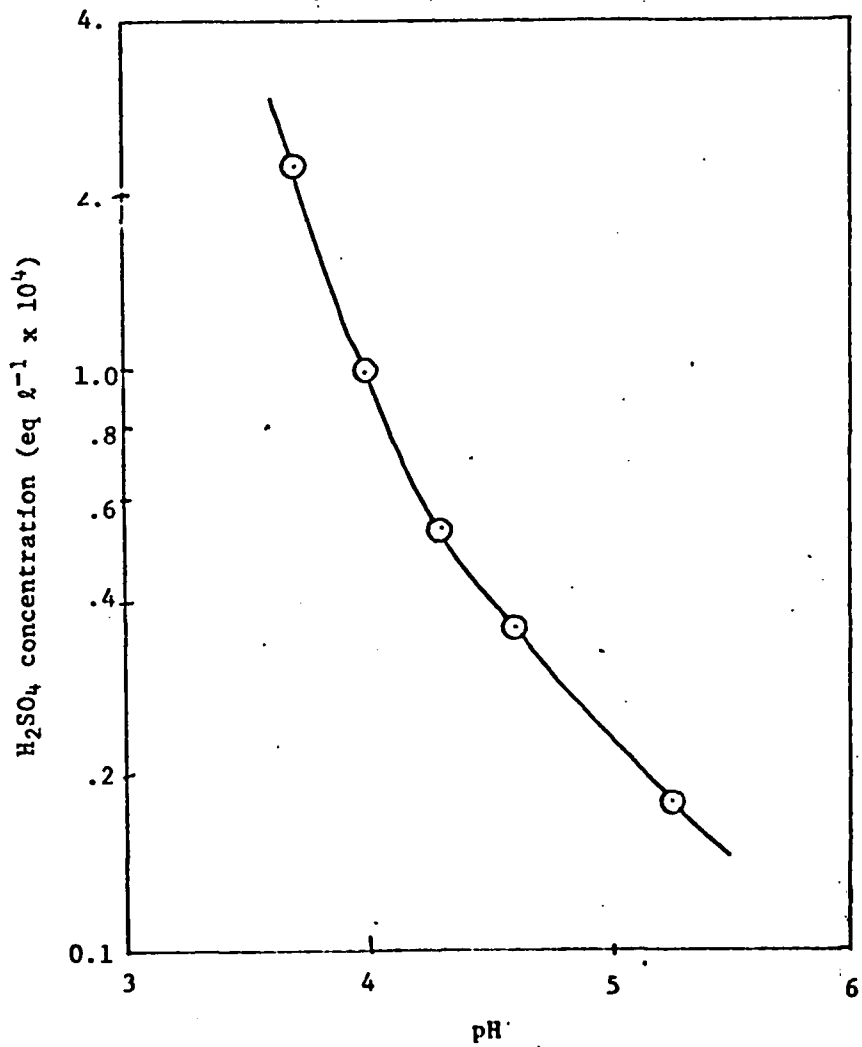


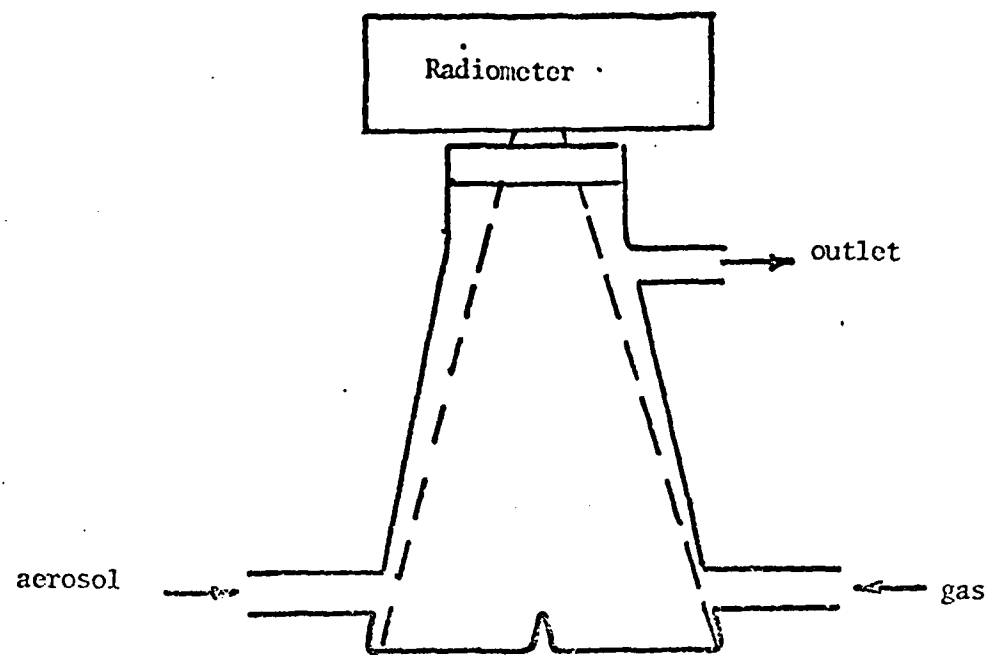
FIGURE 3. CONCENTRATION OF H_2SO_4 vs pH.

As mentioned above, the aerosols for these initial studies were generated by means of a compressed air nebulizer (De Vilbis). This generator produces a polydisperse aerosol with a mass median diameter generally in the range of 2-4 μm , depending upon the liquid. However, this generator is easy to employ, and the mass concentration of the aerosol is quite reproducible under the same conditions of flow rate and tank pressure. Nitrogen gas (20 psi) at a flow rate of 3-6 l/min was employed, resulting in a reproducibility of about 5% for sulfuric acid and dibutylphthalate (DBP). In future studies we will also employ mono-disperse aerosols produced from a condensation type generator. We are currently in the process of modifying and testing these generators.

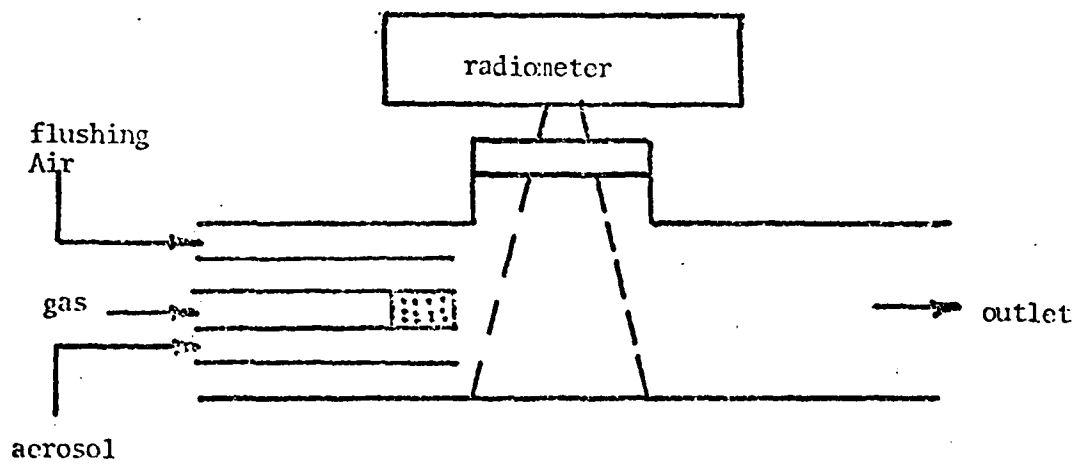
While the reproducibility for H_2SO_4 is 5%, that for chlorosulfonic acid (ClSO_3H) is only 30%. The reason appears to be loss of HCl resulting from the hydrolysis of the ClSO_3H . Ways of eliminating this problem are still being explored.

Screening studies. The initial studies of candidate systems were carried out in the reaction vessels shown in figure 4. In vessel B, the reactive gas is introduced into the aerosol stream by means of a glass frit. Vessel A was the most useful for initial examinations since the field of view of the radiometer (0.1 Sr) encompasses the entire volume, resulting in maximum readings. However, there is some turbulence as well as a large degree of heterogeneity in both the reaction and temperature profiles from the top to the bottom of the vessel. The reaction tube in figure 4 (Vessel B) provides a more uniform but much smaller, reaction volume. In addition, a sheath of flushing air may be employed which serves to prevent accumulation of material on the window and both material and conductive heat transfer to the walls.

The (aerosol/gas) reaction systems surveyed in vessels A and B were decanoic acid/ NH_3 , octylamine/HCl, sulfuric acid/ NH_3 and $\text{NH}_3\text{-H}_2\text{O}$, and chlorosulfonic acid/ H_2O and $\text{NH}_3\text{-H}_2\text{O}$ mixtures. Only the ClSO_3H aerosol gave detectable infrared emission,



Vessel A



Vessel B

Figure 4. Reaction vessels. The dashed lines represent the radiometer field of view.

as shown in figure 5. Similar results are obtained with vessel B, but the emission levels are about 10% of those using vessel A. It should be noted that even the $\text{ClSO}_3\text{H}/\text{H}_2\text{O}$ system produced emission, while the apparently more exothermic $\text{H}_2\text{SO}_4/\text{NH}_3$ and $\text{H}_2\text{SO}_4/\text{NH}_3 - \text{H}_2\text{O}$ systems did not (*vide infra*).

It should also be noted in figure 5 that both the rise and decay times are rather long, considering the fact that the hydrodynamic response time of the flow system is on the order of seconds. This prompted the development of new reaction tube designs, as discussed in the following section.

Reactor System. All of the results presented below have been obtained using the reaction tubes shown in figure 6. The wall-less tube (figure 6a) will be referred to as the "open tube, and the other (figure 6b) as the closed tube. In both tubes the reactive gas stream emerges from the inner tube, the aerosol from the next concentric tube, and the sheathing gas from the outer tube. The principal modifications from earlier designs are the mixing of reactive gas with aerosol via small holes at right angles to the aerosol flow rather than through a glass frit and, for the closed tube, the use of a larger (~2.5 cm diameter) radiometer viewing port. The reaction tube, radiometer and exhaust are mounted in a metal frame shown schematically in figure 7. The entire setup is in a hood, but the exhaust fans in the hood cannot be used since the vibrations and air flow patterns cause excessive interference with the radiometer. For the open tube, a configuration employing a 4 inch diameter exhaust hose and auxillary fan located outside the hood has proved effective. Arrangements involving cone-shaped vacuum exhausts were not effective. The radiometer is on a traverse for accurate and reproducible positioning, and thermistor probes may be inserted in the gas stream at variable locations.

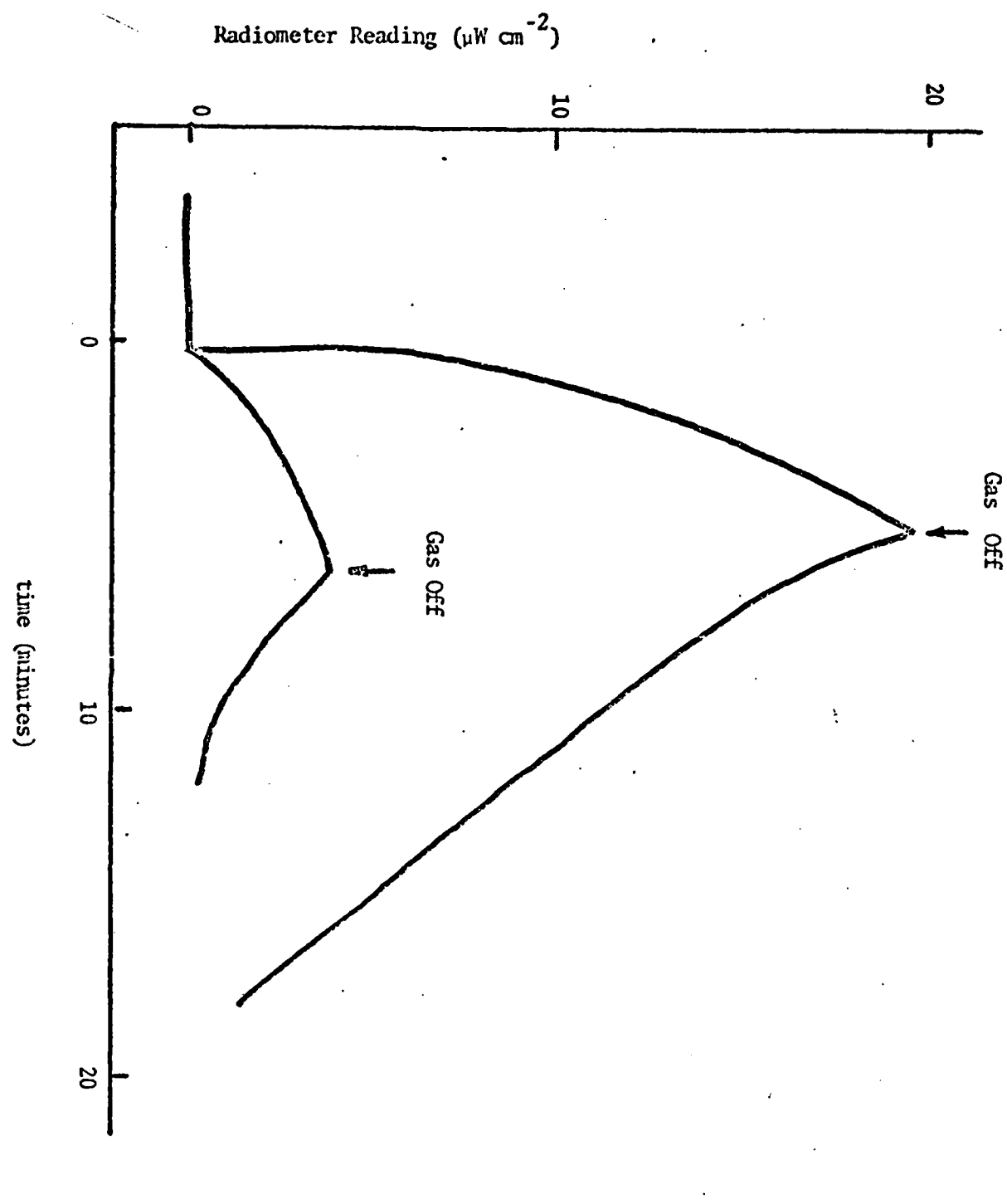
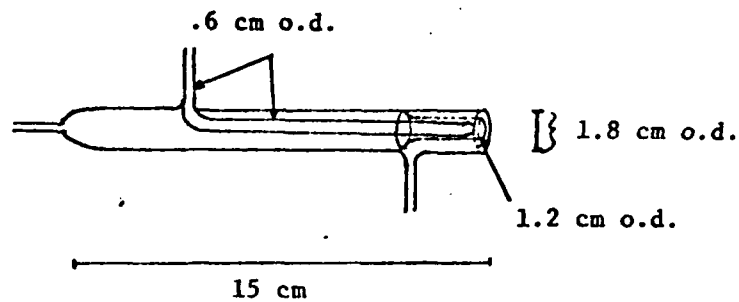


Figure 5. Reaction of ClSO_3H with $\text{NH}_3/\text{H}_2\text{O}$ (upper curve) and H_2O (lower curve) in vessel A.
The reactant gas was turned on at time zero.

(a)



(b)

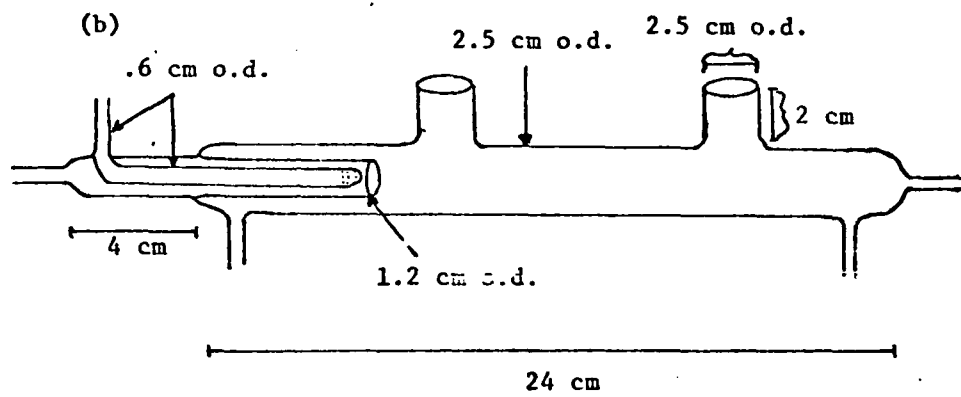


Figure 6.

GAS-AEROSOL REACTION TUBES.

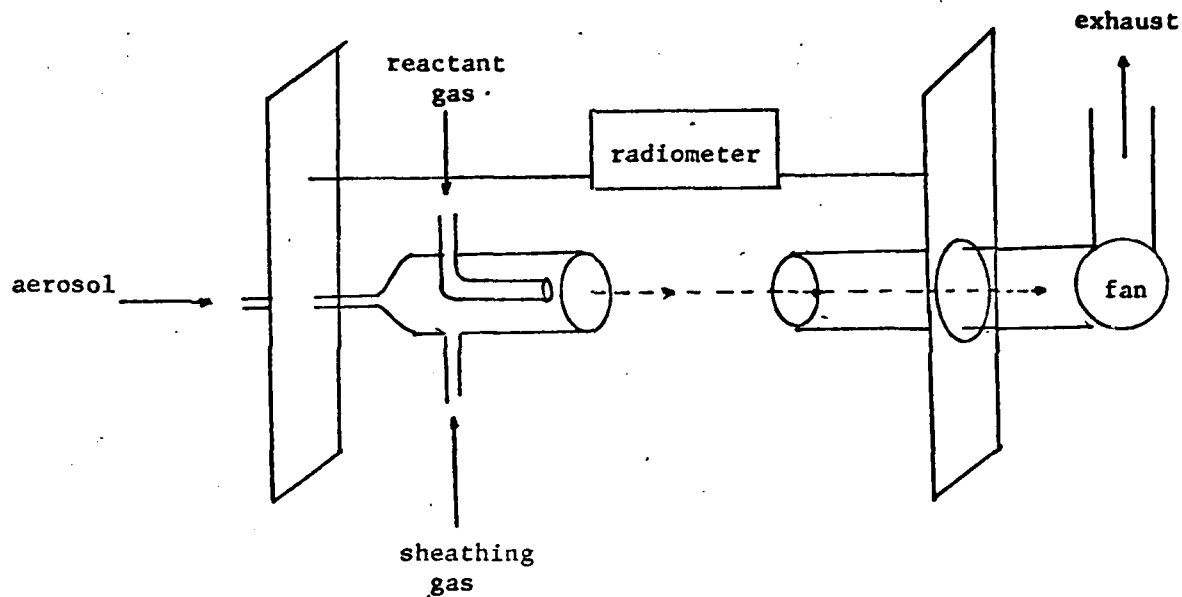


Figure 7. SCHEMATIC DIAGRAM OF REACTION SYSTEM.

The reaction conditions employed in this study are given in Table I. The reactions listed are meant only to show the stoichiometry and not to imply anything concerning the extent or sequence of reaction.

TABLE I. REACTIONS AND CONDITIONS.

A. Reactions (aerosol underlined).

1. $\text{ClSO}_3\text{H} + \text{H}_2\text{O} \text{ (g)} \longrightarrow \text{H}_2\text{SO}_4 + \text{HCl} \text{ (g)}$
 $\text{H}_2\text{SO}_4 + 2\text{NH}_3 \text{ (g)} \longrightarrow (\text{NH}_4)_2\text{SO}_4$
2. $\text{H}_2\text{SO}_4 + 2\text{NH}_3 \text{ (g)} \longrightarrow (\text{NH}_4)_2\text{SO}_4$
3. $\text{RCOOH} + \text{NH}_3 \text{ (g)} \longrightarrow \text{RCOONH}_4$
4. $\text{RNH}_2 + \text{HCl} \text{ (g)} \longrightarrow \text{RNH}_3\text{Cl}$

B. Conditions.

1. Flow rates (l/min):
 - a. sheathing gas, 0.75
 - b. reactive gas, 0.75
 - c. aerosol; ClSO_3H , 5.4; all others 3.4

2. Concentrations (g/m^3):

- a. NH_3 , 20
- b. H_2O , 25
- c. HCl , 8
- d. aerosol; DBP, 5.1; ClSO_3H , 8.0; H_2SO_4 , 1.0

Gas-aerosol reactions. Using the earlier reaction vessel designs (vide supra), only the $\text{ClSO}_3\text{H-NH}_3$ or H_2O reaction gave detectable infrared emission. However, using the present closed reaction tube (figure 6b), emission from all of the reaction systems listed in Table II was observed. We believe this increase in sensitivity results from better mixing geometry and a more favorable radiometer field of view. As with the earlier tube, there is an initial rapid jump in emission upon reaction, followed by a slower increase leveling off after about five minutes. Upon cutoff of the reaction gas, the radiometer decrease took place with a half-life also on the order of five minutes. Since the linear flow velocity of the gas-aerosol stream is on the order of 40 cm sec^{-1} , heating of the glass wall of the reaction vessel seemed to be contributing to the emission. This was confirmed by simultaneous radiometer (R) and temperature (T) measurements using the thermistor probe. A plot of R vs. T is shown in figure 8 for the closed tube (figure 8a). The large hysteresis is indicative of wall effects. Nonetheless, the closed tube is still quite useful for screening studies due to its higher sensitivity. For example, there seems to be a rough correlation between the level of infrared emission and the enthalpy of reaction (Table II). The $\text{ClSO}_3\text{H-H}_2\text{O}$ reaction seems to be an exception, although more quantitative studies are required. These studies may be carried out using an open tube vessel (vide infra).

TABLE II. GAS-AEROSOL REACTION SYSTEMS.

| Aerosol | Gas | ΔH^a | IR ^b |
|--------------------------------|-----------------------------------|---------------------|-----------------|
| octanoic acid | NH ₃ | 21 | w |
| octylamine | HCl | 30 | wm |
| H ₂ SO ₄ | NH ₃ | 65 | -- |
| | NH ₃ /H ₂ O | 64 | m |
| ClSO ₃ H | H ₂ O | 0-40 ^c | ms |
| | NH ₃ /H ₂ O | 96-114 ^c | s |

- a. Estimated heats of reaction in kcal per mole of aerosol material.
- b. Indicates infrared emission (w=weak, m=medium, s=strong).
- c. Upper figure includes heat of hydration of reaction products.

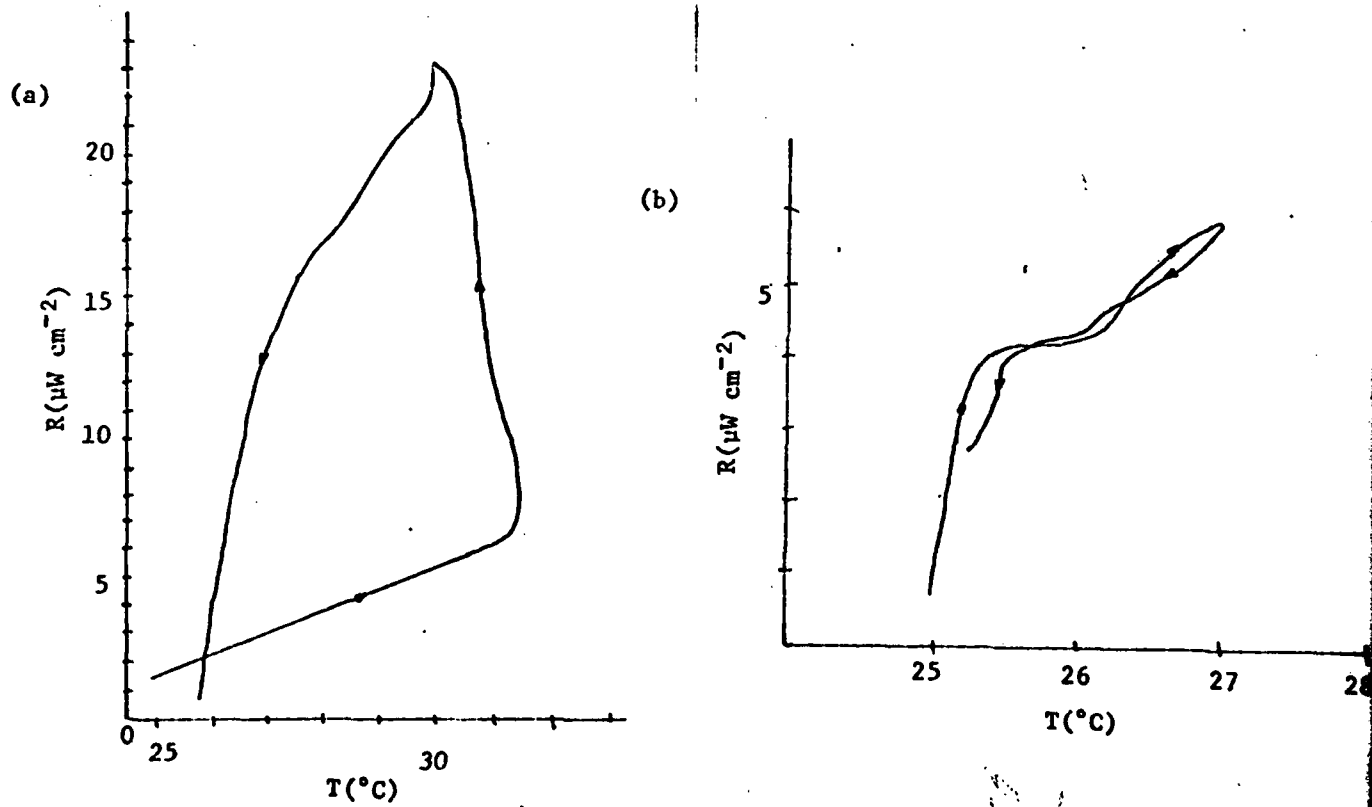


Figure 8. Radiometer reading (R) vs probe temperature (T) for (a) closed tube and (b) open tube (see text).

In order to help eliminate effects due to wall heating, an open tube was employed (figure 6b). That this system is indeed superior to the closed tube in this regard is shown by the rapid response to the introduction and withdrawal of the reactant gas (figure 9) and the lack of R vs. T hysteresis (figure 8b). It should be noted that the flow of reactant gas carrier was not changed. The carrier gas could be led through the reactant gas supply or could bypass it. The open tube does suffer from the disadvantage of being more susceptible to external perturbation such as wind currents and vibrations. Note the noise levels in figure 9.

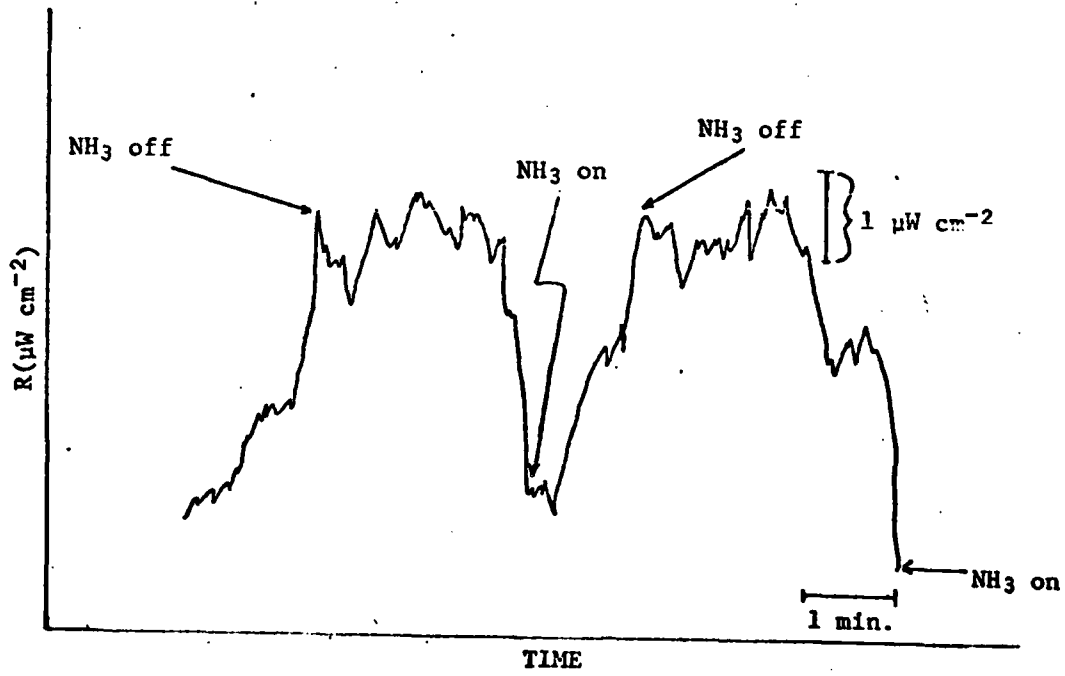


Figure 9. Radiometer response vs time for the $\text{NH}_3/\text{H}_2\text{O}-\text{ClSO}_3\text{H}$ gas-aerosol reaction. The introduction and cutoff of reactant gas is denoted by arrows (see text).

Of course, this was recorded with a 3 sec time constant, and a 100 sec time constant could be used to determine steady-state levels. However, the observed range of measured power per unit area (R) with the open tube is about $1-10 \mu\text{W cm}^{-2}$ com-

pared with current "background" levels of about $1 \mu\text{W cm}^{-2}$. We plan to attempt other modifications to both increase the collected radiation and to decrease the influence of environmental background variations. These include the addition of a controlled enclosure and reflectors. Thus far, emission from the reaction of $\text{NH}_3/\text{H}_2\text{O}$ gas has been observed with both ClSO_3H and H_2SO_4 aerosols.

In order to obtain information on the extent of reaction in the gas stream, temperature-distance (d) profiles were obtained. The distance d is measured from the end of the open tube. The $\text{ClSO}_3\text{H}/\text{NH}_3/\text{H}_2\text{O}$ reaction system was employed, and control heating experiments were performed using DBP. This was done since heating of ClSO_3H without reaction is difficult. In future, it will be better to use H_2SO_4 or some other aerosol as our principal test system so that both reaction and heating experiments can be performed on the same aerosol. The DBP aerosol was heated by passing it through a large diameter tube wrapped with heating tape. The aerosol temperature was varied by controlling the voltage to the heating tape. In this case, the time response is slower due to heating of the reaction tube, so steady-state readings were used. The results to date are somewhat rough and not very extensive. They indicate that the reaction system stream stays "hotter" a bit longer than the heated stream, 3-4 cm vs. 2-3 cm, respectively. In the reaction system, some problems due to accumulation of incompletely reacted aerosol on the probe may occasionally arise. However, the present results serve to demonstrate the potential utility of the method.

Of particular interest are the results of some limited measurements of the R-T response at a fixed distance, nominally 0.5 cm. The heated DBP aerosol yields a $R/\Delta T$ value of $\sim 1 \mu\text{W cm}^{-2} \text{ }^\circ\text{K}^{-1}$, while the $R/\Delta T$ value for the $\text{ClSO}_3\text{H}/\text{NH}_3/\text{H}_2\text{O}$ system is $\sim 2 \mu\text{W cm}^{-2} \text{ }^\circ\text{K}^{-1}$.

As a basis for comparison of the measured power per unit area (R), equation (iv) may be employed.

$$R = 4 \epsilon \sigma T^3 \Delta T \Omega/\pi$$

(iv)

Here ϵ is the emissivity and Ω is the radiometer field of view (solid angle) which is occupied by the object. Assuming a blackbody ($\epsilon=1$) with $T = 298^\circ\text{K}$ and $\Omega = 0.1 \text{ Sr}$, R should increase by about $20 \mu\text{W cm}^{-2}$ for each 1°K rise in temperature. Thus, this latter figure is 10% of the expected blackbody emission ($20 \mu\text{W cm}^{-2} \text{ }^\circ\text{K}^{-1}$). In fact, it is even greater since the gas stream does not occupy the entire radiometer field of view, and should be compared with a value of about $10 \mu\text{W cm}^{-2} \text{ }^\circ\text{K}^{-1}$. This value of 20% of blackbody, if confirmed, is quite high considering the emissivity of air.

Infrared spectral studies. As indicated above, essentially all of the emitted radiation is collected in the present studies. Naturally, it will also be important in later stages of this study to examine the spectral distribution of the emitted radiation. This will in general require an increase in sensitivity, methods for which are currently under investigation (vide supra). However, two IR interference filters centered at 8.0 and $10.6 \mu\text{m}$ with a $0.36 \mu\text{m}$ bandpass were screened using the ClSO_3H aerosol. Emission intensities of about 10% (relative to no filter) were observed with both filters. This result is quite encouraging for future spectral studies.

The temperature probe (thermistor) can give incorrect readings in the reaction stream as noted above. In addition, the higher emissitivity of the reacting vs. heated aerosol may indicate a (transient) droplet temperature which is higher than that of the air (carrier gas) stream. For these reasons, as well as for instantaneous determination of the reaction product(s) and extent, an in-situ method is desired. An infrared spectrum of the aerosol stream should in principle be capable of providing this information. To investigate the feasibility of this method, IR spectra of DBP and ClSO_3H aerosols were obtained on a Perkin-Elmer 621 Infrared spectrophotometer using the cell shown in figure 10a fitted with NaCl windows.

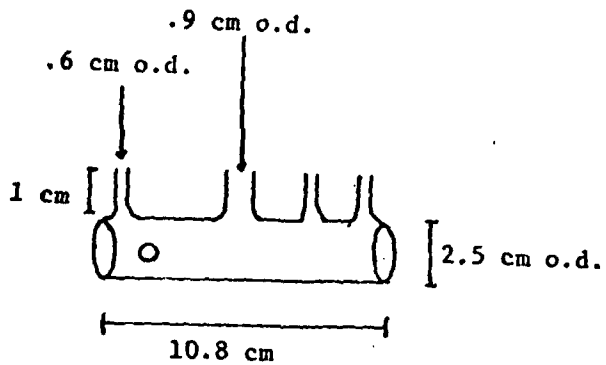


Figure 10a. Cell for obtaining infrared spectra of an aerosol stream.

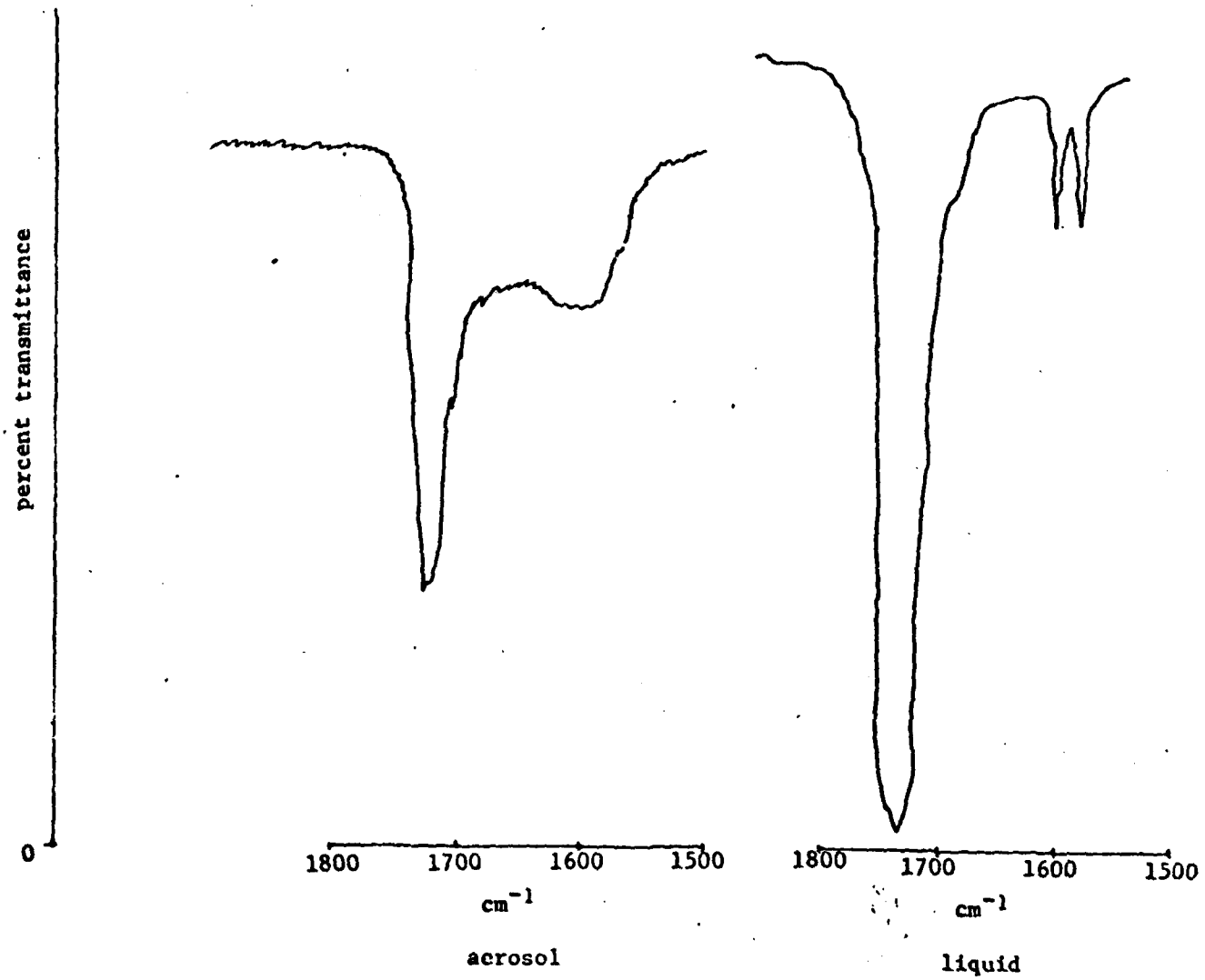


Figure 10b. Infrared spectra of DBP neat liquid and aerosol.

A spectrum of the carbonyl stretching region of the DBP aerosol compared with that of neat DBP is shown in figure 10b. The shape alteration is caused by Mie scattering. The main problem is that even this limited portion of the spectrum takes many minutes to scan, and required the use of an expanded scale. Fluctuations in the output of the aerosol generator, which are virtually impossible to avoid, are sufficiently large to mask the small changes in band envelope due to temperature changes. However, we have demonstrated that in situ IR spectra of aerosols are readily obtained, and believe that the use of Fourier Transform Infrared (FTIR) spectra will yield usable results. Some FTIR experiments are planned for the future.

SUMMARY

Detectable levels of infrared emission have been observed from carboxylic acid, amine, and sulfuric acid gas-aerosol reaction systems, as well as from the very effective reaction of chlorosulfonic acid aerosol with ammonia gas and water vapor. This has been made possible by the development of suitable reaction tubes. Wall heating effects have been minimized by the use of a wall-less reaction system. Significant emission levels corresponding to 20% of blackbody have been observed with the ClSO_3H aerosol, double that of a heated aerosol. Preliminary infrared spectral studies indicate that it should be possible to both measure the spectral dependence of the emitted radiation and to determine aerosol temperature from infrared transmission spectra.

FILMED

2-8